Pharmacokinetic and Biodistribution Profile of Recombinant Human Interleukin-10 Following Intravenous Administration in Rats with Extensive Liver Fibrosis

Heni Rachmawati,[1,2] Leonie Beljaars,[1] Catharina Reker-Smit,[1] Anne-miek M. Van Loenen-Weemaes,[1] Werner I. Hagens,[1] Dirk K. F. Meijer,[1] and Klaas Poelstra[1]

Received January 13, 2004; accepted June 30, 2004

Purpose. Because interleukin-10 (IL-10) seems a promising new antifibrotic drug, we investigated the pharmacokinetic and biodistribution profile of this potent therapeutic cytokine in rats with extensive liver fibrosis (BDL-3). IL-10 receptor expression was also determined in relation to these aspects.

Methods. To study the pharmacokinetic and biodistribution of IL-10, rhIL-10 was labeled with 125-iodine. Plasma samples of ^{125}IrhIL-10 were obtained over a 30-min time period after administration of radiolabeled-cytokine to BDL-3 and normal rats. The tissue distribution was assessed 10 and 30 min after i.v. administration of ^{125}IrhIL-10. IL-10 receptor expression was determined by immunohistochemical staining and RT-PCR technique.

Results. The ^{125}IrhIL-10 plasma curves followed two-compartment kinetics with a lower AUC in BDL-3 rats as compared to control. Plasma clearance and distribution volume at steady state were larger in BDL-3 rats. Tissue distribution analysis in normal rats showed that ^{125}IrhIL-10 highly accumulated in kidneys. In BDL-3 rats, the liver content of ^{125}IrhIL-10 increased by a factor of 2, whereas kidney accumulation did not significantly change. Immunohistochemical staining and RT-PCR analysis showed that IL-10 receptor was clearly upregulated in BDL-3 rat livers.

Conclusions. In normal rats, ^{125}IrhIL-10 rapidly disappears from the circulation, and the kidney is predominantly responsible for this. In BDL-3 rats, the liver largely contributes to this rapid plasma disappearance, probably due to an increase in IL-10 receptor expression. The extensive renal clearance of IL-10 *in vivo* may limit a clinical application of this cytokine for the treatment of chronic liver diseases. To optimize the therapeutic effects of IL-10 in hepatic diseases, alternative approaches that either decrease renal disposition or that further enhance hepatic delivery should be considered.

KEY WORDS: cytokine; extensive liver fibrosis; IL-10 receptor; immunohistochemical staining; rhIL-10.

[1] Department of Pharmacokinetics and Drug Delivery, University Centre for Pharmacy, University of Groningen, 9713 AV Groningen, The Netherlands.

[2] To whom correspondence should be addressed. (e-mail: H.Rachmawati@farm.rug.nl)

ABBREVIATIONS: AUC, area under the plasma concentration-time curve; AUMC, area under the first moment curve; Clp, plasma clearance; Cl_{12}, clearance from central to peripheral compartment; k_{10}, elimination rate constant from the central compartment; k_{12}, rate constant of transfer from central to peripheral compartment; k_{21}, rate constant of transfer from peripheral to central compartment; V_1, volume of distribution in compartment one; V_2, volume of distribution in compartment two; Vss, volume of distribution at steady state.

INTRODUCTION

Interleukin 10 (IL-10), an endogenous cytokine, was initially discovered in 1989 and became known as a cytokine synthesis inhibitory factor for T lymphocytes (1–3). IL-10 is produced by a number of cell types including Th0 and Th2 $CD4^+$ T cells, $CD5^+$ B cells, thymocytes, keratinocytes, and macrophages (1–7). In addition to the production by immune cells, other cell types in other organs can also produce IL-10. The liver is a major source of this cytokine during septic conditions. IL-10 can be synthesized by several cell types within the liver. Hepatocytes, Kupffer cells, and stellate cells all have been reported to produce IL-10 in response to various stimuli (4–14). Because of its potent anti-inflammatory properties, IL-10 has been explored as an antifibrotic cytokine. A new treatment of this chronic disease could be quite relevant because, to date, no effective pharmacological treatment is available for this disease. Recent reports indicate that IL-10 is able to modulate hepatic fibrogenesis, normalize serum ALT, improve histology, and reduce liver fibrosis in patient receiving treatment (4,15,16).

The pharmacokinetics of IL-10 during liver diseases, however, has not been evaluated yet. In healthy human volunteers, intravenous administration of this cytokine resulted in a rapid disappearance from the circulation. The kidney contributed significantly to this rapid elimination (17–20). This rapid clearance of IL-10 *in vivo* may obviously limit the clinical application of this cytokine. Moreover, the distribution to non-target tissues and its multiple effects in all these tissues also strongly hamper the clinical application of IL-10. In order to optimize the effectivity of IL-10 for the treatment of chronic liver diseases such as liver fibrosis, it is essential to know more about the pharmacokinetic of this cytokine during this disease. In the current study, therefore, we determined the pharmacokinetic and organ distribution of IL-10 in rats with extensive liver fibrosis and compared it to normal rats. In addition to this, receptor expression profile determines the success of treatment with exogenous IL-10. Therefore, we also determined IL-10 receptor expression in various organs and in particular in the diseased livers both at the protein and the mRNA level.

MATERIALS AND METHODS

Animals

Specific pathogen-free male Wistar rats, purchased from Harlan (outbred strain, Zeist, The Netherlands), were used in this study. The rats received a standard diet and were housed under standard laboratory conditions. To induce liver fibrosis, rats were subjected to bile duct ligation (BDL) as described by Kountouras *et al.* (21), under anesthesia with 40% O_2:60% N_2O combined with 0.5% isoflurane (Abbot Laboratories Ltd, Queensborough, Kent, UK). Three weeks after the ligation (BDL-3), rats were used for further experiments. Because previous studies did not reveal any difference between untreated animals and animals receiving a sham operation 3 weeks after surgery, we decided to use untreated animals as a control group.

The study as presented was approved by the Local Committee for Care and Use of Laboratory Animals and was

0724-8741/04/1100-2072/0

performed according to strict governmental and international guidelines on animal experimentation.

Radiolabeling of rhIL-10

Five microgram of recombinant human IL-10 (rhIL-10, PeproTech EC Ltd., UK) with a specific activity of about 5×10^5 units mg^{-1} was labeled with 125-iodine (^{125}I) according to the method described by Mather and Ward (22). Prior to each experiment, free ^{125}I was removed by gel filtration using a PD-10 column (Amersham Pharmacia Biotech, Uppsala, Sweden), by eluting with phosphate buffer (0.2 M, pH 7.4) to obtain dosing preparation with less than 5% free ^{125}I.

Pharmacokinetic Study

Normal and BDL-3 rats were anaesthetised with 0.4 $ml \cdot kg^{-1}$ intramuscular Hypnorm (Fentanyl/Fluonisone, Janssen Animal Health, Buckinghamshire, UK) and diazepam (i.m. 2 $mg \cdot kg^{-1}$). The carotid artery was cannulated for rapid blood sampling and the catheter was kept filled with heparin solution (5000 IE $\cdot ml^{-1}$) between samplings to prevent clotting. During experiment, the body temperature of animals was maintained at 37°C by placing them on a thermostatic pad. Each group of normal or BDL-3 rats consisted of 4 rats, but during experiment one rat of BDL-3 group died and was excluded from the study.

A single tracer dose ($\pm 10^6$ cpm) of ^{125}IrhIL-10 was injected intravenously via the penis vein. The blood samples (0.5 ml per time point) were removed from the carotid artery and collected into 1.5 ml eppendorf vials containing 5 μl heparin (5000 IE $\cdot ml^{-1}$ saline; Leo Pharma BV, The Netherlands) at the following time points after injection: 2, 5, 10, 15, 20, and 30 min. Blood samples were then centrifuged (7000 × *g*, 5 min, at room temperature) to obtain plasma. One hundred microliters of plasma was treated with an equivalent volume of 20% trichloroacetic acid (TCA) solution and the mixture was vortexed and centrifuged for 5 min. By TCA treatment, ^{125}IrhIL-10 as well as non-radioactive rhIL-10 is precipitated, whereas radioactive iodine [^{125}I] coupled to low molecular weight proteins or free ^{125}I remains dissolved. The radioactivity in both TCA-precipitated pellets and supernatants was counted separately with a gamma-counter (Riastar Gamma Counting System, Packard Instrument Company, Meriden, CT, USA). The radioactivity of TCA-precipitated pellet represented the IL-10-bound radioactivity (^{125}IrhIL-10). The degradation product of ^{125}IrhIL-10 or free ^{125}I were indicated by radioactivity in the supernatant. The total radioactivity in the plasma was calculated from the total plasma volume. The total radioactivity within the TCA-precipitated pellet was plotted as a function of time to estimate the pharmacokinetic profile as well as all other pharmacokinetic parameters of ^{125}IrhIL-10. All calculated data are presented as mean ± SD.

Pharmacokinetic Analysis

Pharmacokinetic analysis of the plasma concentration vs. time of ^{125}IrhIL-10 was performed using the computer program Multifit (version 8/2000, developed by Dr. J. H. Proost, University Center for Pharmacy, Groningen, The Netherlands). The plasma concentration curves of ^{125}IrhIL-10 were fitted from 2 to 30 min with the Marquardt algorithm and constant relative error variance model (weighting). An iterative two-stage Bayesian population analysis was applied to obtain the population pharmacokinetic parameters of ^{125}IrhIL-10 in normal and BDL-3 rats, using a separate analysis for both groups. This analysis results in estimates for the mean and standard deviation of each parameter. Initial estimates were obtained from a standard two-stage analysis. It was demonstrated that the final population pharmacokinetic parameters were independent of these initial estimates (23). In addition, the data were fitted to a one- and a two-compartment model. The goodness of fit then was assessed by Akaike Information Criterion (AIC), examination of residual variances (CVres), and visual inspection. Visual inspection of the individual data was performed to check the validity of our population analysis. The goodness of fit was best for the two-compartment model, and the following scheme is proposed (Fig. 1).

The pharmacokinetic parameters calculated from the proposed model for distribution volume at steady state and plasma clearance are defined as:

$$V_{ss} = (\text{Dose}*\text{AUMC}_{0-\infty})/[\text{AUC}_{0-\infty}]^2$$

$$\text{Clp} = \text{Dose}/[\text{AUC}_{0-\infty}], \text{ for this study the dose is set to 100\%.}$$

Biodistribution Study

BDL-3 and normal rats, under anesthesia with 40% O_2: 60% N_2O combined with 0.5% isoflurane, received a single tracer dose ($\pm 10^6$ cpm) of ^{125}IrhIL-10 intravenously via the penis vein. Four rats per group were used for each biodistribution study. The organ distribution of ^{125}IrhIL-10 was assessed at 10 and 30 min after administration. At those times, rats were sacrificed and blood samples (±1 ml) were taken by heart puncture and collected into 1.5 ml heparinized tubes. Concurrently, various organs were removed, rinsed with saline, and weighed. Small pieces of these tissues were subsequently weighed and placed into special test tubes and radioactivity was measured. Plasma samples were obtained as described above. The plasma level of ^{125}IrhIL-10 was determined after adding an equal volume of 20% TCA. The amount of ^{125}IrhIL-10 radioactivity in urine was also measured by collecting the urine that was present in the bladder by puncture of the bladder at the time of sacrifice. In this urine, total radioactivity as well as TCA-precipitated radioactivity was determined. The latter reflects protein-bound radioactivity. The radioactivity in each sample was counted us-

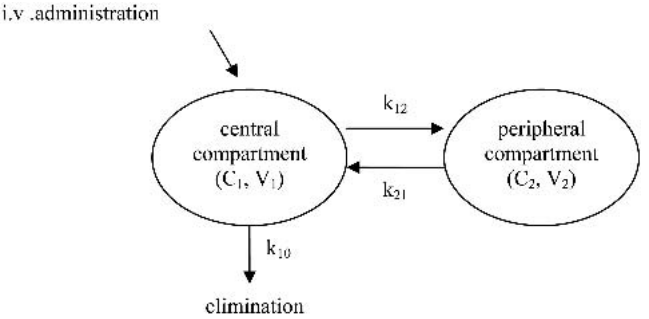

Fig. 1. Proposed two-compartment pharmacokinetic model for IL-10.

ing a gamma-counter. The total radioactivity per organ was corrected for the blood-derived radioactivity in that organ. This correction factor was calculated from organ distribution studies with human serum albumin (HSA), a protein that remains in the blood during the time frame of this experiment (24). All measured data are presented as mean ± SD.

Statistical Analysis

All data were subjected to an unpaired, two-tailed distribution student *t* test. Differences were considered significant at p less than 0.01.

IL-10 Receptor Expression

Protein Expression of IL-10 Receptor

The expression of IL-10 receptor in liver, lung, kidney, and spleen of normal and BDL-3 rats was determined by immunohistochemical staining. The cryostat sections of these organs (4 μm) were fixed in acetone for 15 min. IL-10 receptor was stained with rabbit polyclonal anti IL-10 receptor antibody (Santa Cruz, CA, USA, Biotechnology, Inc.) diluted in PBS, overnight at 4°C. Horseradish peroxidase-conjugated goat polyclonal anti rabbit immunoglobulin (DAKO, Carpinteria, CA, USA) was applied as a secondary step (2 h, at room temperature). After washing, sections were stained with horseradish peroxidase-conjugated rabbit polyclonal anti-goat immunoglobulin (DAKO), 1 h at RT. The peroxidase activity was subsequently visualized with 3-amino-9-ethylcarbazole (AEC; Sigma Chemical Co., St. Louis, MO, USA) for 20 min, and sections were counterstained with hematoxylin (Fluka Biochemica, Buchs, Switzerland) for 2 min. The sections then were mounted in Kaisers glyserin-gelatin (Merck KGaA, Darmstadt, Germany).

Gene Expression of IL-10 Receptor

Total RNA Isolation. Total RNA was isolated from livers of normal and BDL-3 rats with TRIzol reagent according to a standard protocol of the manufacturer (Life Technologies, Carlsbad, CA, USA). DNAse treatment was performed with the DNA-free kit (Ambion, Inc., Austin, TX, USA). The quantity of RNA in the various samples was assessed with the RiboGreen RNA Quantitation Reagent and kit (Molecular Probes, Eugene, OR, USA) according to standard methods. Integrity of RNA samples was checked by electrophoresis on a 2% agarose gel, and the absence of DNA from the samples was verified by running a PCR on the RNA samples using primers for GAPDH while omitting the reverse-transcriptase step.

RT-PCR. An RT-PCR (Promega, Madison, WI, USA) was performed with 1 μg of total RNA in 25 μl of reaction volume to obtain 25 μl cDNA. This synthesized cDNA was examined using the following set of primers: IL-10 receptor primers (GCCCAGAGACTCTCGATGAC and AAGACCCTTCCTTTCCCAGA), GAPDH primers (CCATCACCATCTTCCAGGAG and CCTGCTTCACCACCTTCTTG). PCR was performed in a volume of 25 μl containing 1.25 μl of cDNA, 50 mM $MgCl_2$, 2.5 μl of 10 times concentrated Taq DNA polymerase buffer (Promega), 10 mM dNTP, 0.5 U of Taq DNA polymerase (Eurogenetec, Seraing, Belgium), and 25 pmol of each primer. IL-10 receptor PCR was performed using the following protocol: 5 min 95°C followed by 30 cycles 95°C for 30 s, 56°C for 30 s, and 72°C for 30 s, and finally 72°C for 5 min. As a housekeeping enzyme, we used GAPDH (glyceraldehyde-3-phosphate dehydrogenase). GAPDH PCR cycle conditions were 5 min 95°C followed by 26 cycles 95°C for 30 s, 58°C for 30 s, and 72°C for 30 s, and finally 72°C for 5 min.

PCR products were analyzed on 2% agarose-gels stained with ethidium bromide. The signals from different samples were normalized for the expression of GAPDH and quantified with the QuantityOne quantification software (BioRad Laboratories, Hercules, CA, USA). All calculated data are presented as mean ± SD.

RESULTS

Pharmacokinetic Profile of ^{125}IrhIL-10

To assess the pharmacokinetic profile of IL-10, ^{125}I-labeled rhIL-10 was injected and plasma levels were analyzed for radioactivity after several time intervals.

The log plasma concentration-time curves of ^{125}IrhIL-10 after a single i.v. dose is shown in Fig. 2. The ^{125}IrhIL-10 concentration-time profile for both studied groups exhibited a biphasic kinetic clearance pattern. This was confirmed by analysis of the curves with the pharmacokinetic program Multifit. The Akaike Information Criterion (AIC) of a two-compartment analysis was significantly lower than after fitting with one compartment. The AICs of normal and BDL-3 rats with 1-compartment analysis were –21 and –4 and with two-

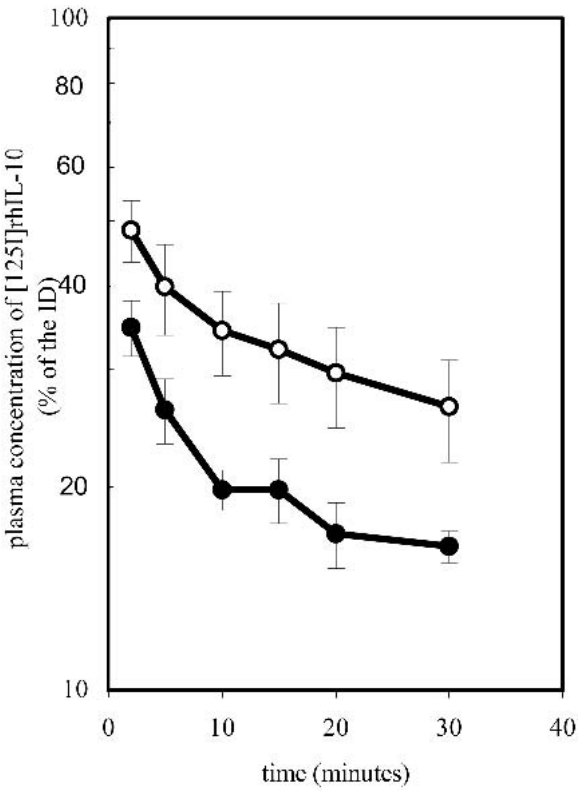

Fig. 2. Log plasma concentration-time plot of a tracer amount of ^{125}IrhIL-10 after intravenous administration in normal (open circles) and BDL-3 rats (closed circles). Plasma levels of ^{125}IrhIL-10 were significantly lower ($p < 0.01$) in BDL-3 rats as compared to normal rats at all time points examined.

Table I. Concentration of Free ^{125}I in Plasma Relative to the Total Radioactivity in Plasma at Indicated Time Intervals After Intravenous Administration of a Tracer Amount of ^{125}IrhIL-10 to Normal and BDL-3 Rats

	Normal rats		BDL-3 rats	
Minutes	Mean (%)	SD (%)	Mean (%)	SD (%)
2	2.24	0	1.74	0.3
5	2.13	0	1.45	0.2
10	1.60	0.4	1.96	0.6
15	2.18	0.6	2.73	2.1
20	3.66	0.7	5.67	2.5
30	6.32	0.8	9.11	4.5

SD, standard deviation of four experiments (normal rats) and of three experiments (BDL-3 rats).

compartment analysis were –48 and –17, respectively. The goodness of fit was also very good with two-compartment analysis, based on the measurement that the CV_{res} for normal and BDL-3 rats was respectively 2.4% and 5.2% with a two-compartment analysis and was respectively 8.8% and 14.9% with a one-compartment analysis. The relatively lower CV% values for the two-compartment analysis are indicative of good model performance. In this pharmacokinetic analysis, we performed a separate analysis for normal and BDL-3 rats assuming differences in liver function between both groups.

The measurements of free ^{125}I in plasma until the last time point (Table I) showed that ^{125}IrhIL-10 was stable in plasma and indicative of almost all of the cytokine was intact. In Table II, the pharmacokinetic parameters of ^{125}IrhIL-10 in both groups were shown. The biexponential pattern of ^{125}IrhIL-10 disappearance from the circulation in normal and BDL-3 rats yielded a rapid initial disappearance rate corresponding to a half-life ($t_{1/2[1]}$) of 1.7 vs. 2 min and a second slow one corresponding to a half-life ($t_{1/2[2]}$) of 52 vs. 75 min. These differences in $t_{1/2}$ between normal and BDL-3 rats, however, were not statistically significant. In contrast, the calculated plasma clearance of ^{125}IrhIL-10 in BDL-3 rats (Fig. 2) was significantly faster than in normal rats. In BDL-3 rats, ^{125}IrhIL-10 disappeared from the circulation for more than 60% within 2 min, and only 34.7 ± 3.3% of the initial dose (ID) was retained in the circulation, whereas in normal rats, 48.4 ± 5.1% of the ID was still present in the circulation 2 min after injection. The plasma disappearances of ^{125}IrhIL-10 at 30 min after injection amounted to more than 75% in normal rats and 80% in BDL-3 rats. On the other hand, the urinous output was very small (protein-bound radioactivity <0.05% of dose, data not shown). In addition, analysis of plasma levels of ^{125}IrhIL-10 over a 30-min time period after administration showed a statistically significant decrease of AUC in BDL-3 rats compared to normal rats (280 ± 67 vs. 390 ± 38). This decrease of AUC in extensive fibrotic rats corresponded with an increase (1.5-fold) of Clp (0.38 ± 0.1 vs. 0.26 ± 0). The increase of Clp of ^{125}IrhIL-10 in BDL-3 rats was proportional with an increase of V_1 of ^{125}IrhIL-10 in BDL-3 rats (1.6-fold). The greater V_1 in this group was also confirmed by a higher

Table II. Pharmacokinetic Parameters of IL-10 After Intravenous Administration of ^{125}IrhIL-10 to Normal and BDL-3 Rats

	Normal rats		BDL-3 rats			
PK parameters	Mean	SD	Mean	SD	p value	p < 0.01
$AUC_{0-\infty}$ (min · % · ml^{-1})	390.36	37.9	279.98	67.2	0.0004	*
$t_{1/2[1]}$ (min)	1.71	0.5	2.03	0.5	0.3865	—
$t_{1/2[2]}$ (min)	52.01	10	75.06	28	0.1997	—
V_1 (ml)	11.29	1.7	17.57	1.7	0.0012	*
V_2 (ml)	7.46	1.8	19.53	7.5	0.0212	—
V_{ss} (ml)	18.77	3.1	37.43	8.2	0.0076	*
Clp (ml · min^{-1})	0.26	0	0.38	0.1	0.0001	*
Cl_{12} (ml · min^{-1})	1.78	0.4	3.03	0.8	0.0052	*
k_{10} (min^{-1})	0.02	0	0.02	0	0.2577	—
k_{12} (min^{-1})	0.16	0.1	0.17	0.1	0.4939	—
k_{21} (min^{-1})	0.24	0.1	0.16	0.1	0.1467	—

SD, standard deviation of four experiments (normal rats) and of three experiments (BDL-3 rats).
* p < 0.01.

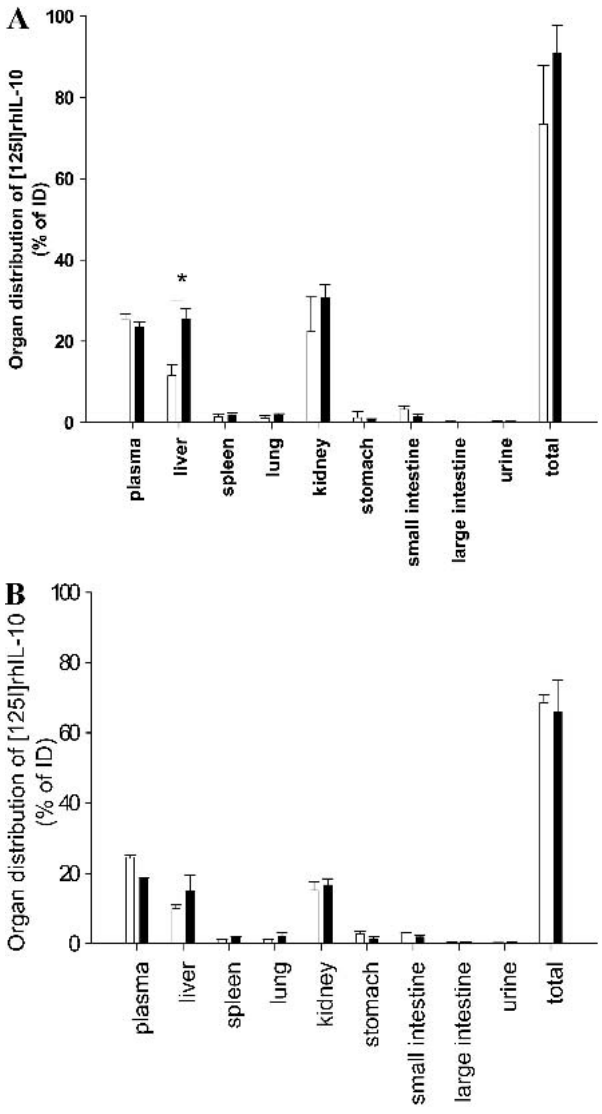

Fig. 3. (A) Organ distribution of ^{125}IrhIL-10, 10 min after intravenous administration of a tracer amount of ^{125}IrhIL-10 in normal (open bars) and BDL-3 (closed bars) rats. (* = p < 0.01). (B) Organ distribution of ^{125}IrhIL-10, 30 min after intravenous administration of a tracer amount of ^{125}IrhIL-10 in normal (open bars) and BDL-3 (closed bars) rats.

ratio of k_{12}/k_{21} in this group (1.06) as compared to normal rats (0.67). It follows that the V_{ss} in BDL-3 rats was larger as well, as shown in Table II.

Tissue Distribution of ^{125}IrhIL-10

Figure 3 shows the tissue distribution of ^{125}IrhIL-10, 10 and 30 min after intravenous administration of a tracer amount of ^{125}IrhIL-10 in normal and BDL-3 rats. At 10 min after administration of ^{125}IrhIL-10, about 70% ID disappeared from the circulation and was mainly found in kidney (23%) and secondly in the liver (11%). The accumulation of ^{125}IrhIL-10 in other tissues and in the urine was less than 5%. In BDL-3 rats, 80% ID of ^{125}IrhIL-10 disappeared from the circulation and we found an increased accumulation of ^{125}IrhIL-10 in the liver (25.43%) in comparison with normal rats, while the renal content did not change. At t = 30 min, a significant increase of hepatic accumulation was still observed. Thus, the liver content of ^{125}IrhIL-10 in BDL-3 rats showed a significant increase at both indicated time points. In contrast, the renal content did not differ between both groups studied (n = 4 per group).

The IL-10 Receptor Expression

The expression of IL-10 receptors in various tissues is shown in Fig. 4. Immunohistochemical staining showed a low constitutive expression of IL-10 receptors in the kidney, liver, spleen, and lung of normal rats. In the kidney, the expression of IL-10 receptor was seen in the glomeruli and on the spindle-shaped cells around blood vessels. In the liver, the expression of IL-10 receptors was observed on fibroblast-like cells in the portal area, whereas in lung staining seemed to be associated with fibroblast cells. The IL-10 receptor in the spleen appeared to be expressed by B cells or T cells, by fibroblast-like cells around blood vessels and by other cells of monocyte presumably macrophage cell-lineage. In BDL-3 rats, IL-10 receptor expression in livers (n = 4) was strongly upregulated, and this was predominantly observed on fibroblast-like structures that are present around the bile ducts. In contrast, an upregulation of IL-10 receptor expression was not observed in the other organs studied. The RT-PCR analysis for the IL-10 receptor as depicted in Figs. 5A and 5B also showed a strong upregulation of this receptor in BDL-3 rat livers (3.21-fold) as compared to normal rat livers.

DISCUSSION

IL-10 has been applied as a therapeutic cytokine in several inflammatory diseases because it has potent anti-inflammatory activities. In the past decade, studies have been initiated to explore the effects of this cytokine on fibrosis (5,7,9,10,11,13,15). A recent study reported that a long-term IL-10 therapy in chronic hepatitis C could decrease disease

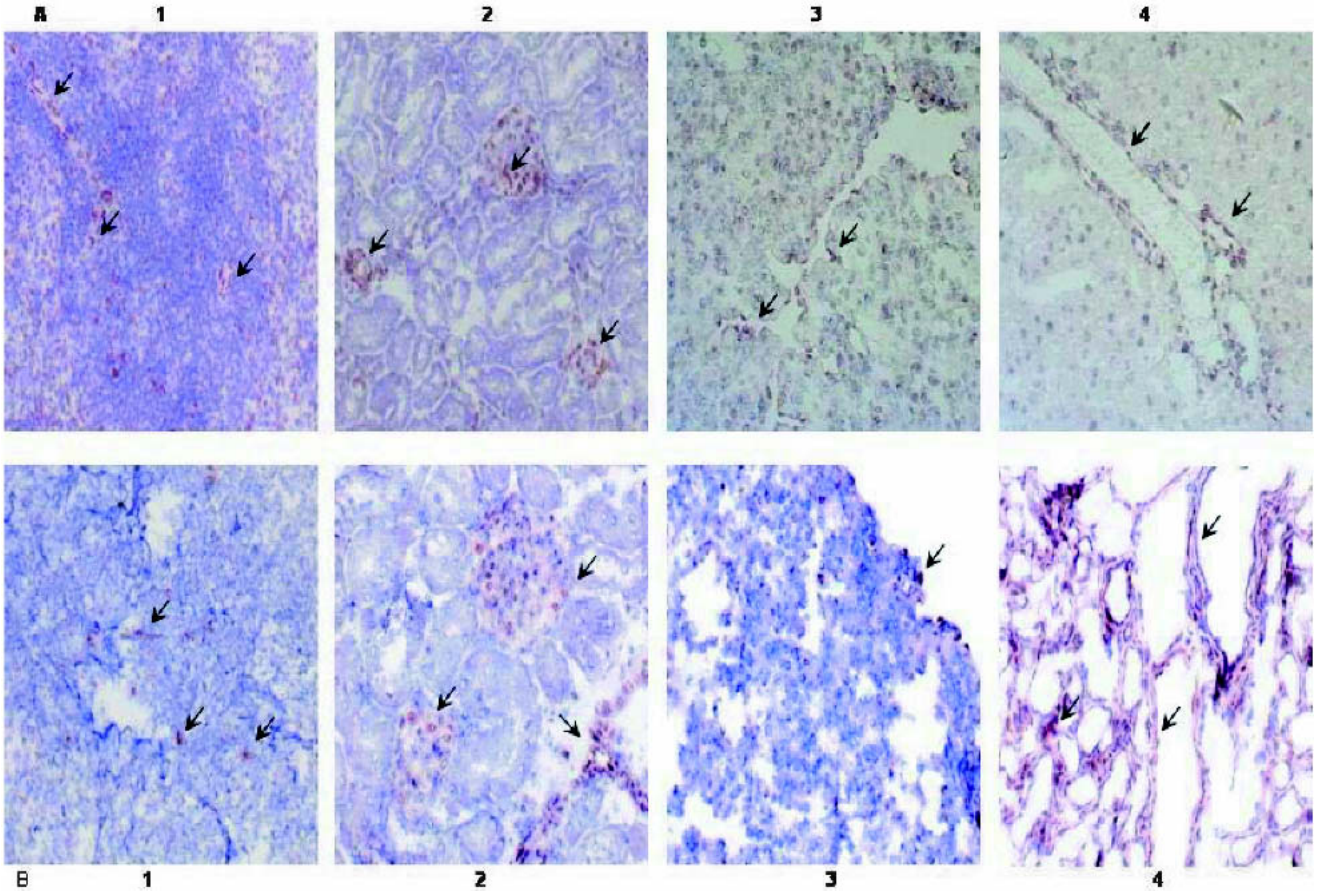

Fig. 4. IL-10 receptor expression in spleen (1), kidney (2), lung (3), and liver (4) of normal (A) and BDL-3 (B) rats. The IL-10 receptor expression (red) is indicated by arrows. It can be seen that the expression of IL-10 receptor is strongly increased in BDL-3 rat livers as compared to normal rat livers (original magnification ×200).

symptoms such as inflammation and fibrotic scores (16). In the same study however, a flare-up of viral levels in the serum was noted, possibly due to the immunosuppressive effect of IL-10. This unwanted effect of the IL-10 therapy is a logical consequence of the pleiotropic activities of IL-10. IL-10 has anti-inflammatory effects on immune-competent cells and the anti-fibrotic effects on fibroblast-like cells. The IL-10 receptor expression found by us on both fibroblast-like cells and immune cells (Fig. 4) clearly reflects this pleiotropism.

Because IL-10 seems to play an inhibitory role during the progression of liver fibrosis and because first attempts to use this cytokine as a therapeutic drug in liver disease are being explored now, we examined the pharmacokinetic profile of this promising cytokine. Although several studies about the pharmacokinetic profile of IL-10 have been reported, this was only examined in healthy individuals or in renal disorder models (17–20), and never related to receptor expression. These reports indicate that IL-10 is rapidly cleared from the circulation by the kidney. This was a non-saturable process, indicating excretion by glomerular filtration. Therefore, a renal dysfunction might largely influence the pharmacokinetic profile of this cytokine, and this requires adaptation of the dose regimen. Yet, impairment of the function of liver and change in receptor expression may alter the overall pharmacokinetic profile of cytokines as well. In the current study, we evaluated the pharmacokinetic and organ distribution of ^{125}IrhIL-10 in rats with extensive liver fibrosis and in normal rats, and also studied its receptor expression. In normal rats, ^{125}IrhIL-10 rapidly disappeared from the circulation after i.v. administration and distributed mainly to the kidney which confirms the other studies (17–20). The very low radioactivity

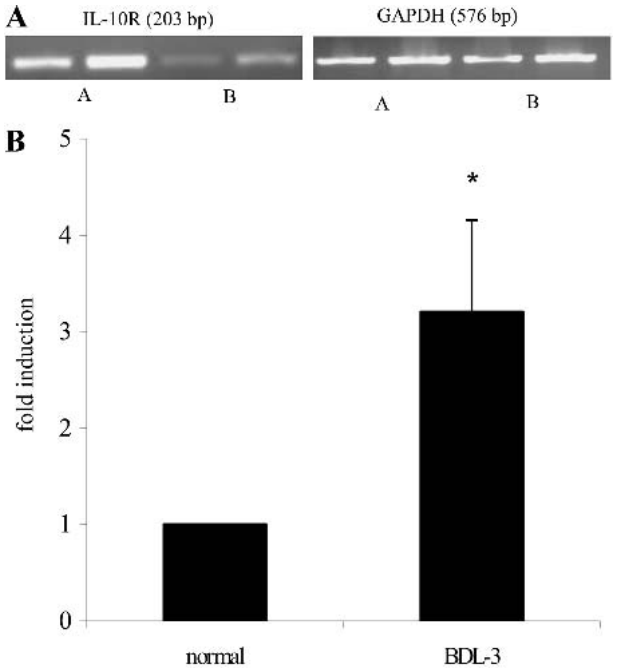

Fig. 5. mRNA levels of IL-10 receptor in BDL-3 (lanes A) and normal rat livers (lanes B). The IL-10 receptor mRNA levels are strongly upregulated in BDL-3 rats (left panel). Right panel shows mRNA levels of GAPDH in BDL-3 (lanes A) and normal rat livers (lanes B). (B) Quantitative evaluation of the RT-PCR products. Note the significant increase of mRNA levels for the IL-10 receptor in BDL-3 rat livers compared to normal rat livers (* = $p < 0.01$).

which was measured in urine showed that ^{125}IrhIL-10 is poorly excreted into the urine. Because IL-10 is a low molecular weight protein (MW as a dimer = 37 kDa), this low urinary excretion suggests that ^{125}IrhIL-10 was rapidly cleared by glomerular filtration and reabsorbed through the renal tubuli. Again, this supports the conclusions from another study (18). However, because normal glomeruli express the IL-10 receptor, receptor binding may also account for the kidney uptake. This constitutive expression of IL-10 receptor did not change in BDL-3, and corresponded with an unchanged renal accumulation of ^{125}IrhIL-10 (Fig. 3). Biological effects in the kidney may therefore be anticipated.

In BDL-3 rats, we observed an altered pharmacokinetic profile of ^{125}IrhIL-10. In this group, the AUC decreased highly significant ($p < 0.01$) compared to normal rats. The higher initial plasma disappearance rate (Clp) and distribution volume of ^{125}IrhIL-10 may account for the decreased AUC in diseased rats. Organ distribution studies with ^{125}IrhIL-10 revealed an increase in hepatic uptake in BDL-3 rats (2-fold). This demonstrated that during liver fibrosis, not only the kidney contributes to the rapid clearance of ^{125}IrhIL-10 from the circulation but also the liver. The size of the liver is enhanced during fibrosis by a factor 2, although the number of hepatic cells may be actually decreased due to the excessive scar formation at this stage. Immunohistochemical staining of IL-10 receptor in several organs revealed a strong upregulation of this receptor expression only in BDL-3 rat livers (Fig. 4). This hepatic increase in receptor expression was also found at the mRNA level (Fig. 5). So, the markedly elevated IL-10 receptor expression in the livers may mediate the observed enhanced hepatic uptake of ^{125}IrhIL-10. This higher uptake of ^{125}IrhIL-10 in fibrotic livers may imply a beneficial effect of IL-10 during this disease. Yet, the high renal clearance of ^{125}IrhIL-10 even during liver fibrosis may limit the efficacy of IL-10 therapies; already 2 min after administration of a bolus dose, 80% has disappeared from the plasma. So, the biodistribution and pharmacokinetic profile of this cytokine seems inappropriate to treat a chronic disease like liver fibrosis. However, the biologic half-life within the target cells is also important and this remains to be elucidated. In addition, the pleiotropic activities of this cytokine and the receptor expression found in non-target cells as shown in our study (Fig. 4) may account for adverse effects on the immune system and the kidney.

To our knowledge, this study is the first report evaluating the pharmacokinetic and tissue distribution profile of IL-10 in an experimental model of liver fibrosis. This liver disease highly influences many pharmacokinetic parameters and distribution of IL-10, and receptor expression for this cytokine is affected as well. The strong influence of liver impairment on these parameters was highly significant (Table II; Figs. 2, 3A, and 5B). All these aspects in turn will influence the pharmacodynamic of IL-10. Our results provide an important background for the rational design of an IL-10 delivery system. A cell-selective delivery of IL-10 to treat chronic liver diseases such as liver fibrosis may further improve its efficacy and reduce its side effects. Apart from a liver-specific form of IL-10 that increases its hepatic antifibrotic effect, one may prevent the dominant renal disposition of the cytokine. Studies are in progress in our institute to address both aspects.

ACKNOWLEDGMENTS

We are grateful to Dr. J. H. Proost, Department of Pharmacokinetics and Drug Delivery, University of Groningen, The Netherlands, for kindly providing Multifit software to analyze the pharmacokinetic data and for helpful discussions. Also, the discussions with Dr. R. J. Kok are appreciated. We thank Mr. J. Hans Pol, Nuclear Department, Academic Hospital Groningen, The Netherlands, for the radiolabeling of IL-10. This project was supported by grant from Islamic Development Bank (IDB), Jeddah, Saudi Arabia.

REFERENCES

1. K. W. Moore, R. D. W. Malefyt, R. L. Coffman, and A. O'Garra. Interleukin-10 and the interleukin-10 receptor. *Annu. Rev. Immunol.* **19**:683–765 (2001).
2. D. Pajkrt, L. Camoglio, M. C. T. Buul, K. de Bruin, D. L. Cutler, M. B. Affrime, G. Rikken, T. van der Poll, J. W. ten Cate, and S. J. van Deventer. Attenuation of proinflammatory response by recombinant human IL-10 in human endotoxemia: effect of timing of recombinant human IL-10 administration. *J. Immunol.* **158**: 3971–3977 (1997).
3. M. Howard, A. O'Garra, H. Ishida, R. D. W. Malefyt, and J. de Vries. Biological properties of interleukin 10. *J. Clin. Immunol.* **12**:239–247 (1992).
4. K. Assadullah and H. D. Volk. Interleukin-10 therapy-review of a new approach. *Pharmacol. Rev.* **55**:241–269 (2003).
5. H. Louis, O. L. Moine, M. Goldman, and J. Deviere. Modulation of liver injury by interleukin-10. *Acta Gastroenterol. Belg.* **66**:7–14 (2003).
6. P. Knolle, J. Schlaak, A. Uhrig, P. Kempf, K. H. M. zum Buschenfelde, and G. Gerken. Human Kupffer cells secrete IL-10 in response to lipopolysaccharide (LPS) challenge. *J. Hepatol.* **22**: 226–229 (1995).
7. K. Thompson, J. Maltby, J. Fallowfield, M. McAulay, H. Millward-Sadler, and N. Sheron. Interleukin-10 expression and function in experimental murine liver inflammation and fibrosis. *Hepatology* **28**:1597–1606 (1998).
8. P. A. Knolle, A. Uhrig, U. Protzer, M. Trippler, R. Duchmann, K. H. M. zum Buschenfelde, and G. Gerken. Interleukin-10 expression is autoregulated at the transcriptional level in human and murine Kupffer cells. *Hepatology* **27**:93–99 (1998).
9. K. C. Thompson, A. Trowern, A. Fowell, M. Marathe, C. Haycock, M. J. Arthur, and N. Sheron. Primary rat and mouse hepatic stellate cells express the macrophage inhibitor cytokine interleukin-10 during the course of activation in vitro. *Hepatology* **28**: 1518–1524 (1998).
10. H. Louis, J. L. van Laethem, W. Wu, E. Quertinmont, C. Degraef, K. van den Berg, A. Demols, M. Goldman, O. Le Moine, and A. Geerts. and J. Deviere. Interleukin-10 controls neutrophilic infiltration, hepatocyte proliferation, and liver fibrosis induced by carbon tetrachloride in mice. *Hepatology* **28**:1607–1615 (1998).
11. S. C. Wang, M. Ohata, L. Schrum, R. A. Rippe, and H. Tsukamoto. Expression of interleukin-10 by in vitro and in vivo activated hepatic stellate cells. *J. Biol. Chem.* **273**:302–308 (1998).
12. D. F. Fiorentino, A. Zlotnik, T. R. Mosmann, M. Howard, and A. O'Garra. IL-10 inhibits cytokine production by activated macrophages. *J. Immunol.* **147**:3815–3822 (1991).
13. P. Mathurin, S. Xiong, K. K. Kharbanda, N. Veal, T. Miyahara, K. Motomura, R. A. Rippe, M. G. Bachem, and H. Tsukamoto. IL-10 receptor and co-receptor expression in quiescent and activated hepatic stellate cells. *Am. J. Physiol. Gastrointest. Liver Physiol.* **282**:G981–G990 (2002).
14. R. M. Weber-Nordt, M. A. Meraz, and R. D. Schreiber. Lipopolysaccharide-dependent induction of IL-10 receptor expression on murine fibroblasts. *J. Immunol.* **153**:3734–3744 (1994).
15. D. R. Nelson, G. Y. Lauwers, J. Y. N. Lau, and G. L. Davis. Interleukin 10 treatment reduces fibrosis in patients with chronic hepatitis C: A pilot trial of interferon nonresponders. *Gastroenterology* **118**:655–660 (2000).
16. D. R. Nelson, Z. Tu, C. Soldevila-Pico, M. Abdelmalek, H. Zhu, Y. L. Xu, R. Cabrera, C. Liu, and G. L. Davis. Long-term interleukin 10 therapy in chronic hepatitis C patients has a proviral and anti-inflammatory effect. *Hepatology* **38**:859–868 (2003).
17. R. D. Huhn, E. Radwanski, S. M. O'Connell, M. G. Sturgill, L. Clarke, R. P. Cody, M. B. Affrime, and D. L. Cutler. Pharmacokinetics and immunomodulatory properties of intravenously administered recombinant human interleukin-10 in healthy volunteers. *Blood* **87**:699–705 (1996).
18. S. R. Andersen, L. J. Lambrecht, S. K. Swan, D. L. Cutler, E. Radwanski, M. B. Affrime, and J. J. Garaud. Disposition of recombinant human interleukin-10 in subjects with various degrees of renal function. *J. Clin. Pharmacol.* **39**:1015–1020 (1999).
19. P. Chiu, E. Radwanski, G. Tetzloff, A. Monge, and S. Swanson. Interleukin-10 pharmacokinetics in intact and nephrectomized mice. *Eur. Cytokine Netw.* **7**:67–69 (1996).
20. E. Radwanski, A. Chakraborty, S. V. Wart, R. D. Huhn, D. L. Cutler, M. B. Affrime, and W. J. Jusko. Pharmacokinetics and leukocyte responses of recombinant human interleukin-10. *Pharm. Res.* **15**:1895–1901 (1998).
21. J. Kountouras, B. H. Billing, and P. J. Scheuer. Prolonged bile duct obstruction: a new experimental model for cirrhosis in the rat. *Br. J. Exp. Pathol.* **65**:305–311 (1984).
22. S. J. Mather and B. G. Ward. High efficiency iodination of monoclonal antibodies for radiotherapy. *J. Nucl. Med.* **28**:1034–1036 (1987).
23. F. Mentre and R. Gomeni. A two-step interative algorithm for estimation in nonlinear mixed-effect models with an evaluation in population pharmacokinetics. *J. Biopharm. Stat.* **5**:141–158 (1995).
24. L. Beljaars, B. Weert, H. Bonnema, P. Olinga, G. M. Groothuis, G. Molema, D. K. F. Meijer, and K. Poelstra. Albumin modified with mannose 6-phosphate: a potential carrier for selective delivery of antifibrotic drugs to hepatic stellate cells. *Hepatology* **29**: 1486–1493 (1999).